A REVIEW OF THE DEVELOPMENT, MICROSTRUCTURE AND PROPERTIES OF NEW Al-Li ALLOYS

ICAS-86-2.7.2

Edgar A. Starke, Jr.
School of Engineering and Applied Science
University of Virginia
Charlottesville, Virginia

Abstract

The main purpose of adding lithium to aluminum alloys is to obtain a better combination of low density, high elastic modulus, and high strength -- properties especially attractive for aerospace applications. This paper describes the development of new Al-Li-X alloys, their microstructures and their properties. Emphasis has been placed on Al-Li-Cu and Al-Li-Cu-Mg since the most recent alloys being considered for commercialization are based on these alloy combinations. The Cu and Mg are added to form precipitates which increase strength and ductility. In addition to alloy composition, processing parameters, such as deformation prior to age hardening and the aging temperature, must be tightly controlled if the optimum properties are to be realized. The effect of processing on the microstructure and properties is also discussed.

I. Introduction

Aircraft designers are constantly striving to achieve minimum weight in order to cut fuel consumption and improve overall performance. Reducing the density of structural materials has been shown to be the most efficient solution to this problem (1), Figure 1. Since aluminum alloys make up between seventy and eighty percent of the current aircraft weight, recent alloy development programs have focused on reducing the density of these materials (2). Lithium is the lightest metallic element and has a significant effect on density when alloyed with aluminum, producing a 3% decrease for every weight percent added up to the limit of solid solubility (3). In addition, a concomitant increase in elastic modulus has been reported for both binary and complex alloy systems (4). Unfortunately, these beneficial effects are usually accompanied by a significant decrease in ductility and toughness making the simple alloys unsuitable for many structural applications.

The potential advantages of lithium additions to aluminum were first recognized by LeBaron who obtained a patent on the Al-Cu-Li-X alloys in 1945. Subsequently, the Al-Cu-Li alloy 2020 was commercially produced and in 1957 was used on the United States Navy RA 5C Vigilante; however, concerns about the alloy's brittle behavior, and production problems, thwarted further use and 2020 was withdrawn from commercial production in the 1960's (5). More recently, rising fuel costs and the demand to produce more fuel efficient and higher performance aircraft has led to renewed interest in Al-Li alloys.

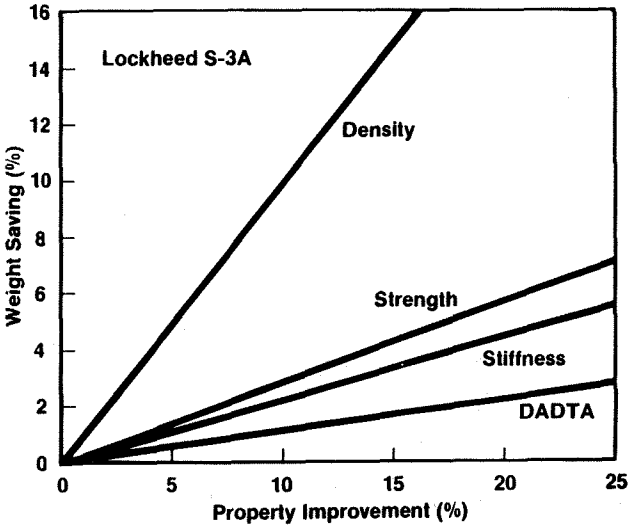

Figure 1. The influence of various properties on structural weight savings of the S-3A aircraft which is typical of many studies (1).

This paper will describe the major causes of the low ductility and fracture toughness of simple Al-Li alloys and how they may be overcome by selective alloy additions and processing procedures.

II. Microstructure and Fracture of Al-Li

When Al-Li alloys containing more than 1 wt.% lithium are quenched from the single-phase field and aged at a temperature considerably below the solvus, homogeneous precipitation of the metastable phase delta prime (Al 3 Li) occurs. The metastable precipitates are coherent with the matrix, and, although they can be sheared by moving dislocations, they impede their motion and, consequently, greatly improve the strength over that of unalloyed aluminum. During aging, heterogeneous precipitation of the equilibrium delta (AlLi) phase also occurs, normally at grain boundaries. The AlLi precipitates consume the lithium from the surrounding region and produce a lithium-depleted, precipitate-free-zone (PFZ) adjacent to the grain boundary. The three microstructural features just described are shown in the bright field transmission electron micrograph of Figure

2a and sheared Al_3Li in the dark field transmission electron micrograph of Figure 2b.

The major strengthening effect of Al_3Li is due to their long-range ordered structure which is reduced when the precipitates are sheared by dislocations.

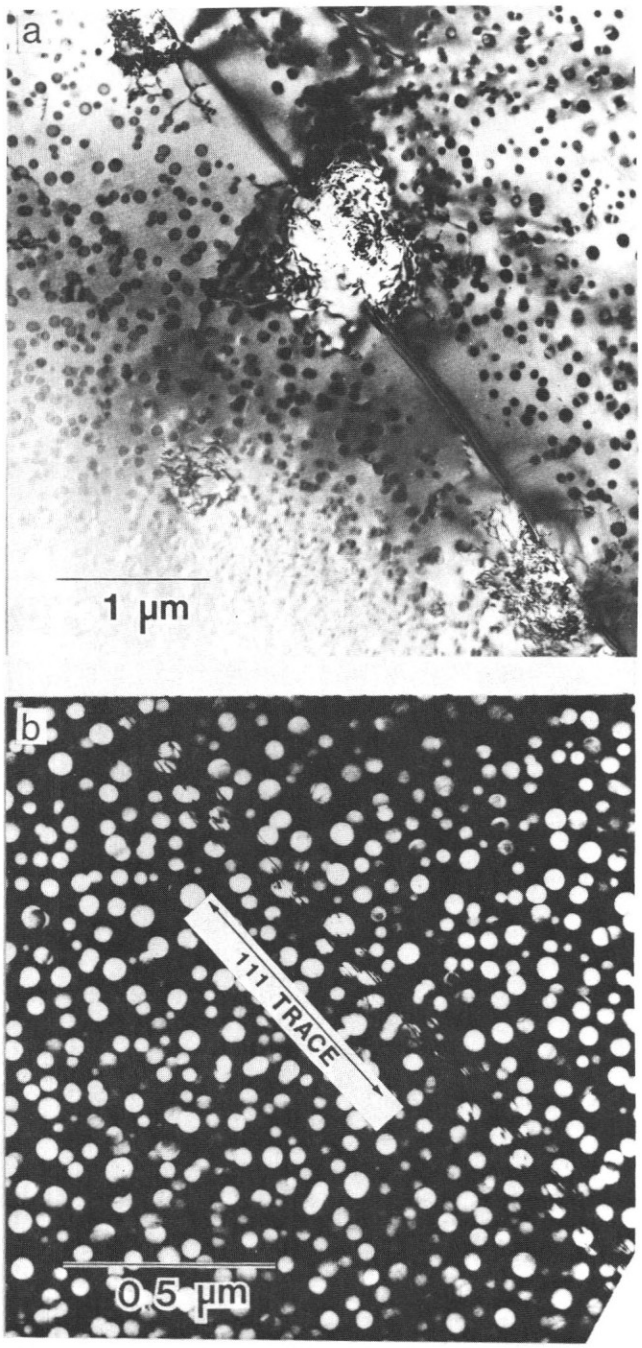

Figure 2. TEM's of Al-2Li aged 24h at 392F. (a) Bright field showing Al_3Li in matrix, AlLi at grain boundary and PFZ, (b) Dark field showing sheared Al_3Li that occurs during deformation.

This results, successively, in a local decrease in resistance to further dislocation motion and a concentration of slip, Figure 3a. The PFZ adjacent to the grain boundary is also weaker than the matrix and can likewise be a region of concentrated slip, Figure 3b. Both types of concentrated slip produce stress concentrations at grain boundaries and grain boundary triple junctions and low energy intergranular or intersubgranular fracture. These failure modes are shown schematically in Figure 4a, and by the scanning electron micrograph of Figure 4b. In addition to these types of strain localization problems, the old 2020 alloy had a large volume fraction of coarse constituents and intermetallic particles. These coarse particles have been shown to have an adverse effect on fracture toughness (6) and numerous investigators have demonstrated that decreasing the Fe content in high strength aluminum alloys decreases the volume fraction of large insoluble phases and increases the toughness (7).

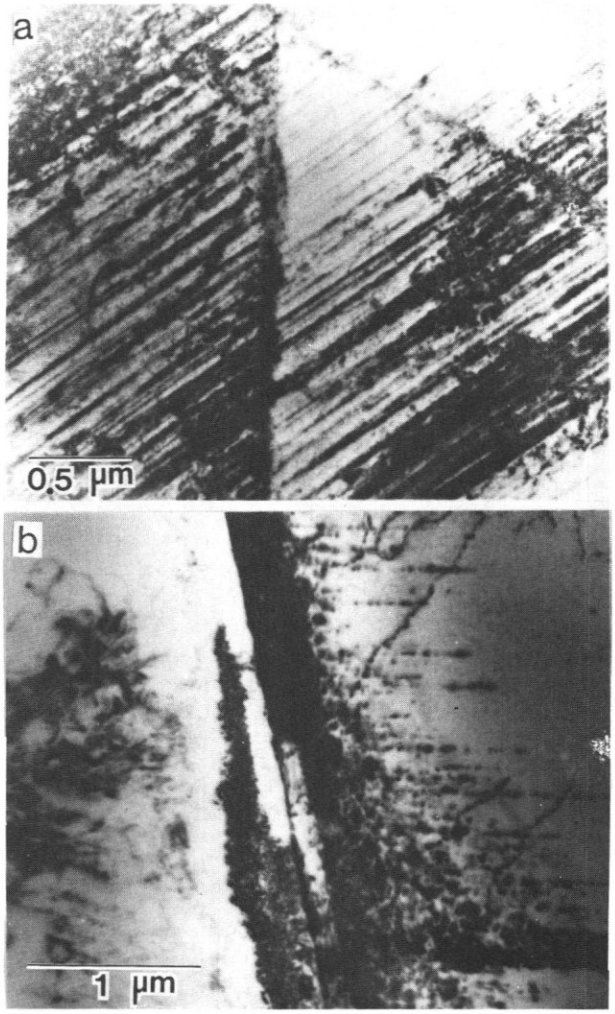

Figure 3. TEM's of deformed Al-2.3Li (a) Aged 4h at 392F showing localized deformation in the matrix, (b) aged 10h at 374F showing localized deformation in the PFZ.

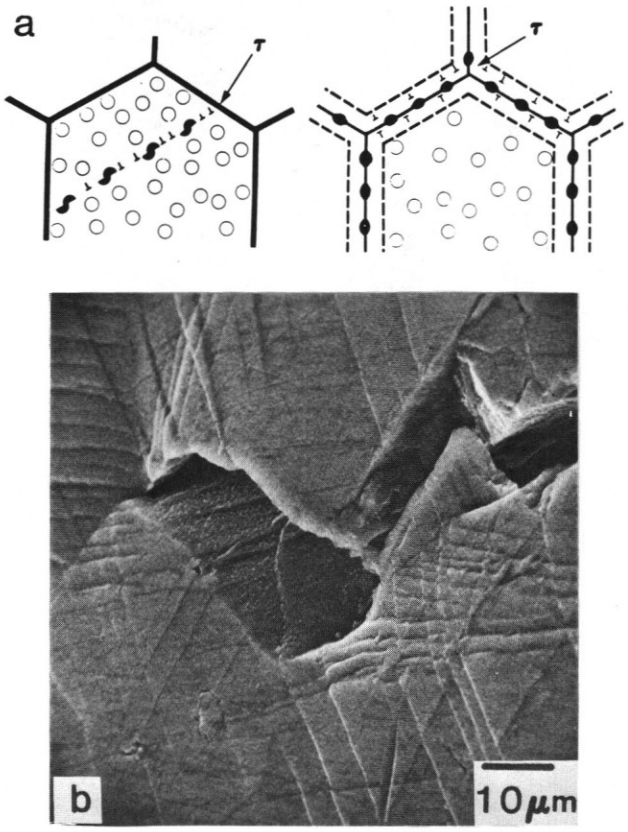

Figure 4. (a) Schematic representation of deformation leading to fracture in Al-Li alloys, (b) SEM showing intense planar slip and intergranular fracture in an Al-3Li alloy.

III. Improving Fracture Toughness

Various modifications in alloy chemistry and fabrication techniques have been used in an attempt to improve the ductility and fracture toughness while maintaining a high strength. Essentially three problems have been addressed: (i) the strain localization in the matrix, (ii) coarse precipitates along grain boundaries, their associated PFZ and strain localization in the PFZ, and (iii) the adverse effects of coarse constituents and intermetallic particles. Strain localization due to particle shearing can be minimized by overaging to produce incoherent precipitates, by reducing the grain size, or by adding alloying elements which promote homogeneous deformation (8). Overaging is impractical in Al-Li alloys because the coherency strains of the Al_3Li strengthening precipitates are small (9), and coherency loss does not occur during aging (10). In addition, precipitation of the equilibrium AlLi, or other equilibrium phases, at grain boundaries results in problem (ii), i.e., the formation of wide PFZ's at grain boundaries.

A reduction in grain size decreases the slip length and reduces the stress concentrations at grain boundaries and grain boundary triple junctions when deformation is localized within the matrix or PFZ. Small grains also enhance multiple slip at low strains producing more homogeneous deformation. Both of these effects have been shown to increase the ductility in age-hardened aluminum alloys containing coherent matrix precipitates and PFZ's (11). Since the deformation behavior of age-hardened alloys is determined by the nature of the interaction of dislocations with the strengthening precipitates, it can be modified by changes in the type, size, coherency, and distribution of the precipitates present. Consequently, alloying is also a potentially attractive method of eliminating strain localization effects in Al-Li alloys. Control of alloy chemistry may also be used to eliminate problem (iii), i.e., coarse constituents and intermetallic particles.

Many programs which focused on the development of Al-Li-X alloys utilized the basic principles mentioned above. A variety of production methods including rapid solidification and powder metallurgy consolidation (12), mechanical alloying (13), and ingot casting (14,15), have been used. Rapid solidification and mechanical alloying were used as a means of reducing the grain size and extending solid solubility; however, simply reducing the grain size did not have a significant effect on ductility, and advantages of extended solubility were negated by elevated temperature excursions during processing (16). Consequently, once problems associated with ingot casting were overcome, this method appeared the most feasible for the production of large plate and extrusion products.

The effect of a variety of alloying additions on the microstructure and properties of Al-Li alloys have been studied, as well as the effect of certain types of impurities. Iron and silicon contents have been kept to a minimum in order to reduce the detrimental effects of constituent particles. Also, alloying additions that form incoherent precipitates, e.g., Mn, Co, and Ni did not seem to significantly improve the ductility of Al-Li alloys prepared by rapid solidification and powder metallurgy consolidation (17). Although the dispersoids did homogenize the slip in the matrix, they did not eliminate the effect of the PFZ's. Consequently, most programs focused on alloying additions that co-precipitate with the Al_3Li phase, and depending on the processing, precipitate up to the grain boundaries, thus eliminating the PFZ. Copper, Mg, and Zr were shown to be the most attractive additions.

IV. Microstructures of New Al-Li-X Alloys

Copper has a very positive effect on the strength when added to Al-Li alloys, and depending on the composition, may coprecipitate in the matrix with the Al_3Li phase as Al_2CuLi (T1) and/or Al_2Cu (theta prime). Often, as is the case for the new alloy 2090 (Al-2.3Li-2.5Cu-0.14Zr, nominal composition in weight percent), all three phases can occur. Examples of one variant of the Al_2Cu and Al_2CuLi precipitates as they occur in a peak-strength temper of an alloy similar to 2090 are given in Figures 5a and 5b. The partially incoherent T1 and theta prime phases may reduce the extent of strain localization; however, their effectiveness in homogenizing strain depends on their size and distribution which may be controlled by deformation prior to aging. The primary role of deformation is to increase the dislocation density and thereby the number of nucleating sites for heterogeneous precipitation. The effectiveness of the process is related to the interfacial strains of the precipitates, being highly effective for precipitates, e.g., T1 and theta prime, having large interfacial strains. An example of the effect of deformation on the size and distribution of the T1 phase in an Al-Li-Cu alloy is shown in Figure 6.

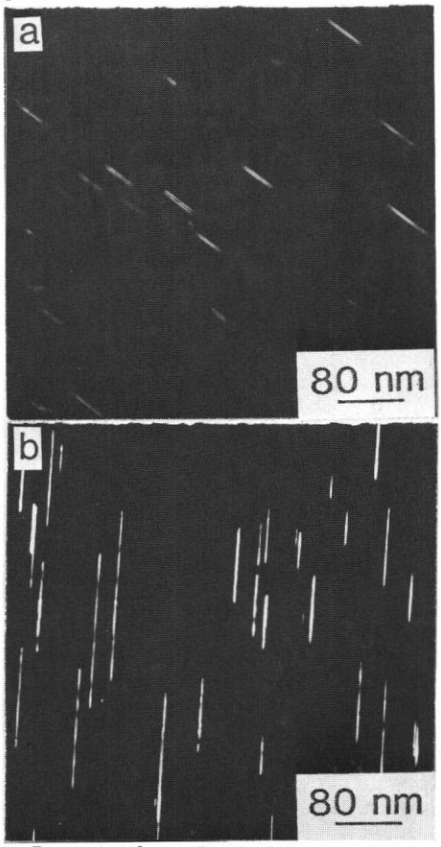

Figure 5. TEM's of Al-Li-Cu alloy. (a) DF of Al_2Cu using the streak associated with precipitates lying on the {100} planes of the matrix, (b) DF of Al_2CuLi using the streak associated with the precipitates lying on the {111} phases of the matrix.

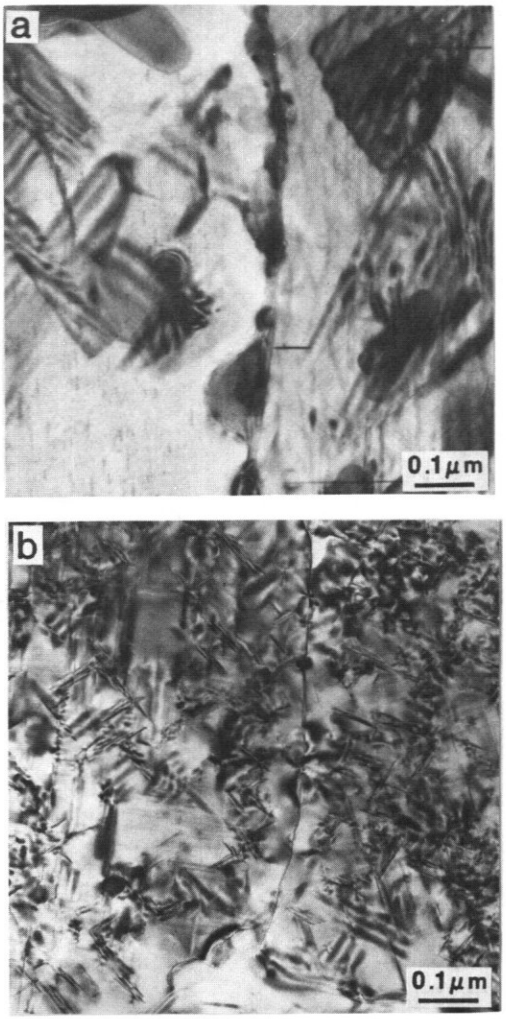

Figure 6. TEM's showing the effect of deformation on nucleation of the Al_2CuLi precipitate (a) undeformed prior to aging, (b) stretched 3% prior to aging.

Other phases, e.g., Al_6CuLi_3 (T2), may form at the grain boundaries in Al-Li-Cu alloys. Cassada et al. (18,19) have recently characterized the grain boundary precipitates in Al-Li-Cu alloys. They found that T2 and a precipitate of unknown composition but exhibiting icosahedral symmetry are the dominate grain boundary precipitates (not AlLi) in alloys of composition similar to 2090. The icosahedral precipitates formed by nucleation and growth over temperatures ranging from 338-968F and were the dominate grain boundary precipitate from 374 to 968F. Below 374F the T2 phase was the dominate grain boundary precipitate. The icosahedral grain boundary precipitates and associated diffraction pattern and the matrix T1 phase are shown in the electron micrograph of Figure 7. Since grain boundary precipitation is competitive with the homogeneous precipitation which occurs in the matrix, it may be minimized by selective control of the aging time and temperature and amount of deformation prior to aging.

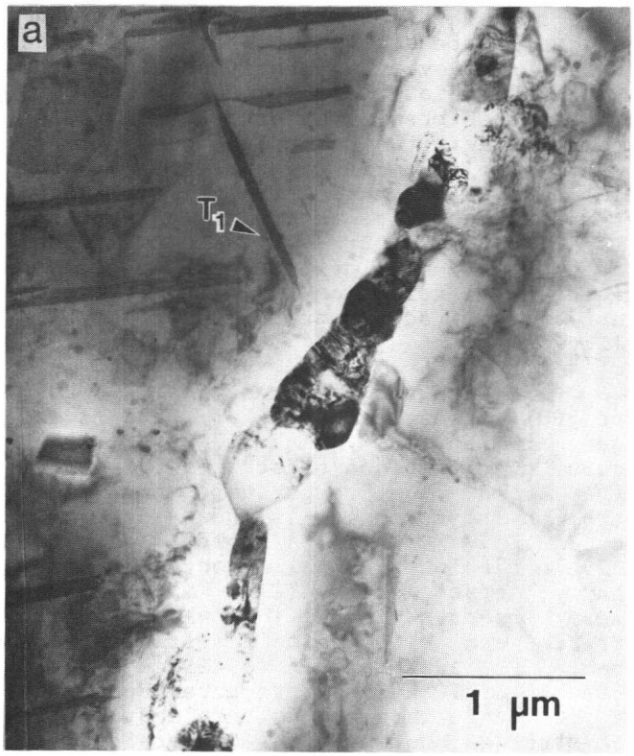

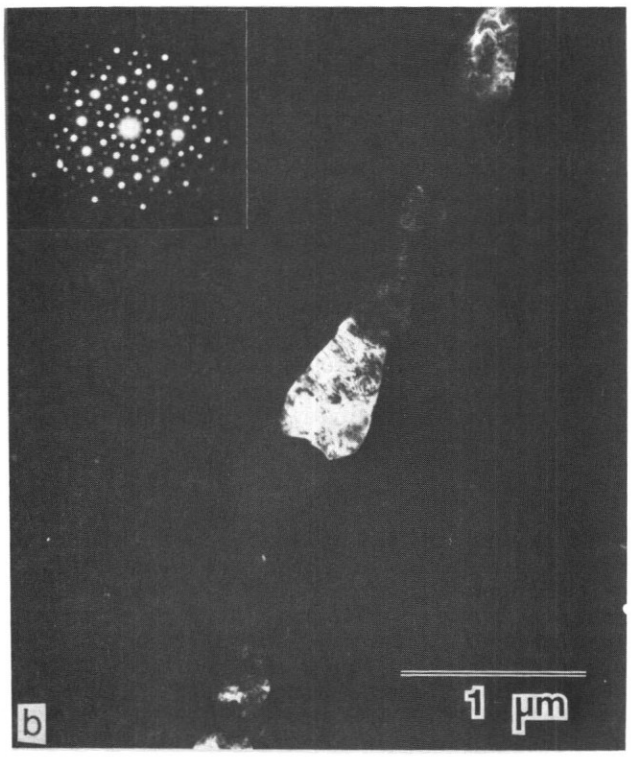

Figure 7. TEM's of Al-2.45Li-2.43Cu-0.18Zr aged 72h at 374F. (a) Bright field showing icosahedral phase at grain boundary and Al_2CuLi (T1) in the matrix, (b) Dark field of icosahedral phase at the grain boundary.

Magnesium additions to Al-Li-Cu alloys may provide a component of solid solution strengthening to the PFZ, and, if present in sufficient quantity, may also coprecipitate with Al_3Li as S" or S' (Al_2CuMg). Since these metastable phases have large coherency interfacial strains, their size and distribution are also sensitive to processing, as observed in Figure 8. In the Al-2.5Li-1.5Cu-1Mg-0.14Zr (nominal weight percent) alloy 8090, the S' phase replaces the T1 that is observed in 2090. However, in the Al-2.3Li-2.0Cu-0.7Mg-0.14Zr alloy 8091, both T1 and S' are present along with the delta prime. The Zr present in all three alloys, 2090, 8090, and 8091, forms the metastable Al_3Zr dispersoid during solidification and/or during ingot preheat and is very effective in inhibiting recrystallization and grain growth during solutionizing treatments (20). Since the Al_3Zr dispersoid is small, spherical, and coherent with the matrix, Figure 9, it has no detrimental effect on fracture toughness. Staley has shown that the Mn and Cr dispersoids are more detrimental to the fracture toughness of 7XXX alloys than are Zr dispersoids (7).

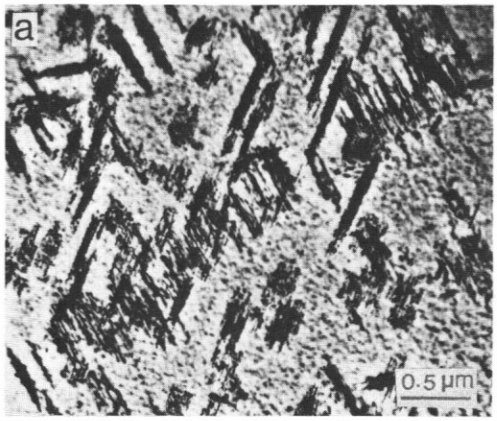

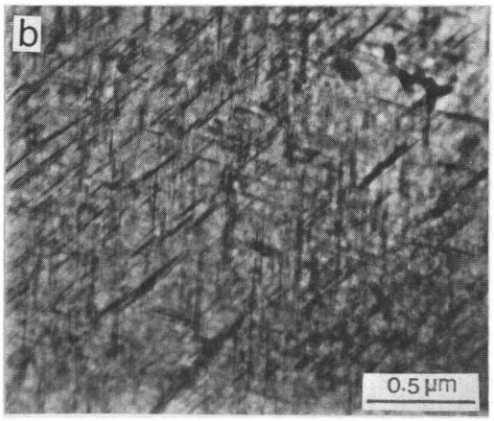

Figure 8. TEM's showing the distribution of Al_2CuMg (S') in an Al-2.7Li-1.5Cu-1Mg-0.15Zr alloy aged 310h at 338F, (a) no stretch before aging, (b) 2% stretch before aging.

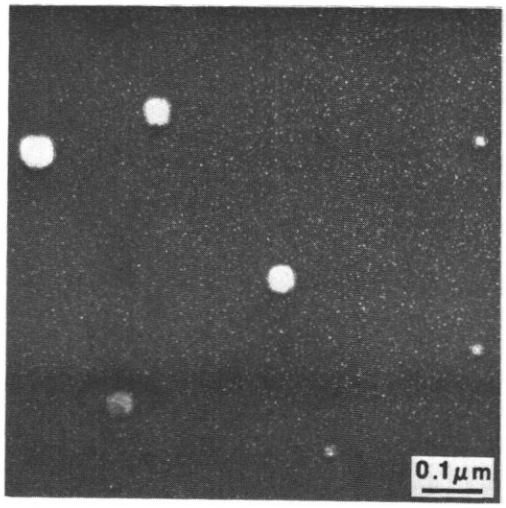

Figure 9. Dark field TEM using a {100} superlattice spot of a solution treated and naturally aged Al-2Li-3Cu-1Mg-0.2Zr alloy. The large participates are Al_3Zr and the smaller ones Al_3Li.

V. Processing for Fracture Resistance

Of all the age-hardenable aluminum alloys, the Al-Li-X alloys are probably the most sensitive to processing. This is most likely due to the very complex nature of the precipitation that occurs in these alloys and the extremely adverse effect that grain boundary precipitates, PFZ's, and shearable precipitates (all of which are affected by processing) have on the fracture behavior. These microstructural features may be more detrimental in Al-Li alloys than in other aluminum alloys because of the occurrence of impurities, such as Na, K, and H, at grain boundaries. The Na and K are normal impurities in Li, and hydrogen levels have been routinely observed to be an order of magnitude higher in Al-Li alloys than in other Al alloys.

Beginning with the as-cast ingot, processing includes an homogenization treatment to reduce segregation, remove low-melting-point phases and thus improve workability. This thermal treatment also serves to precipitate the Zr-dispersoids so that they may perform their role of grain control during further processing. One must be very careful in going to the final homogenization temperature to ensure that the low-melting phases are dissolved before their melting temperatures are reached. A heating rate of 50F/hour from 600F to the normal homogenization temperature of 1010F is frequently used. Homogenization is normally followed by a mechanical working operation for ingot breakdown and shape change, solution heat treatment to put those elements which will participate in the age hardening process in solid solution, and a quench to retain them in solid solution.

Age hardenable aluminum alloys are often stretched after quenching and prior to aging in order to redistribute the residual stresses associated with the quench. However, as mentioned in section IV, deformation prior to aging can also effect the precipitation reaction since those precipitates that have large interfacial strains may nucleate on the dislocations. In addition, precipitation at grain boundaries is greatly affected by the aging temperature. A recent study by Ashton et al. (21) examined the effect of degree of deformation and aging temperature on the fracture properties of Al-Li-X alloys.

Half-inch gauge plates of alloys 2090 and 8091 were stretched 0, 3, and 7% and aged at 250, 297, and 347F for 12-60 hours. The combined effect of stretch age time, and age temperature on yield strength and toughness is shown in Figures 10 and 11. Figure 10a shows that, for 2090 in the longitudinal direction maximum Charpy impact energy (CIE) at a given yield strength is obtained when a high stretch and a low aging temperature are used. For example, if we select a yield strength of 60 ksi, a fracture toughness of 600 in-lb/in(exp2) is obtained using a 7% stretch and an aging temperature of 250F, whereas only 135 in-lb/in(exp2) is obtained for no stretch and a 347F aging temperature. There are, however, obvious practical limits on how high the stretch can be and how long an aging practice at low aging temperature can be tolerated. The effect of stretch is paramount in the the longitudinal direction of 2090. In the long transverse direction, the effect is not as marked, Figure 10b. All age and stretch combinations fall into a narrower band. There is still a toughness benefit in using a 3% stretch but no further improvement in using a 7% stretch.

Alloy 8091, tested in the longitudinal direction, shows the same general trends as 2090, Figure 11a, i.e., stretching and lower aging temperatures are beneficial. However, the effect of aging temperature at a given yield strength is more dramatic. For example, selecting a yield strength of 65 ksi, one can obtain a fracture toughness of 770 in-lb/in(exp2) using a 7% stretch and an aging temperature of 250F, whereas a fracture toughness of 625 in-lb/in(exp2) is obtained using the same stretch but a higher aging temperature of 297F. A fracture toughness of only 105 in-lb/in(exp2) is obtained when no stretch and an aging temperature of 347F is used. This shows that a six- or seven-fold variation in fracture toughness, for the same yield strength, can be obtained by varying the deformation prior to aging and the aging temperature. Figure 11b shows that, unlike 2090, a significant difference in fracture toughness with variations in aging practice is also obtained in the long transverse direction.

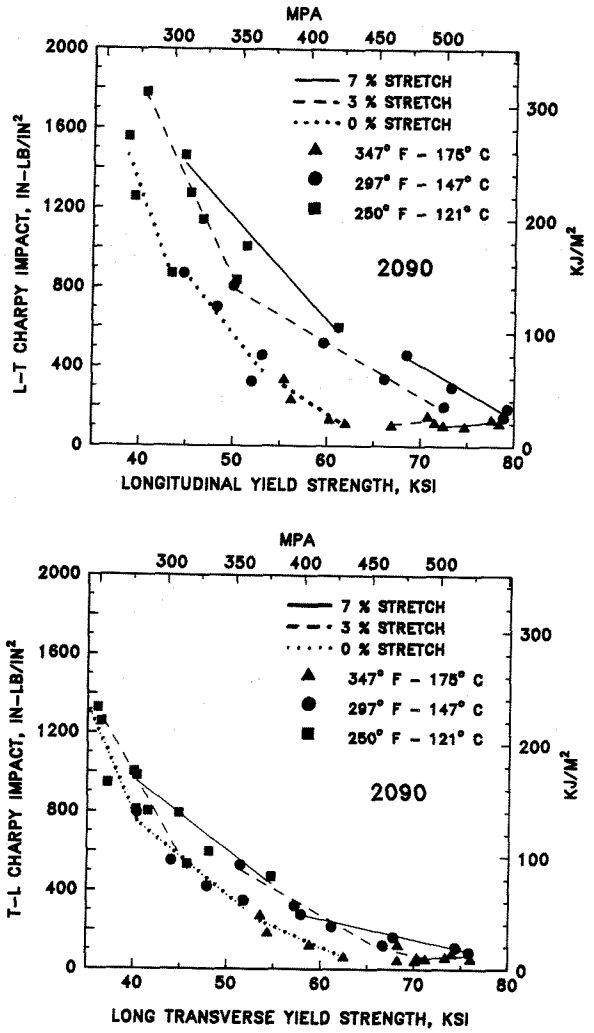

Figure 10. Effect of % stretch and aging practice on the yield strength and Charpy impact energy of 2090 0.50" plate. Plate was solution treated at 1006F. (a) Upper-L, (b) Lower-LT.

The variations in fracture toughness described above can be explained in terms of microstructural variations that accompany changes in both the amount of deformation prior to aging and the aging temperature. In general, the size and volume fraction of grain boundary precipitates decrease with decreasing temperature; and the associated PFZ width decreases with decreasing temperature. As mentioned previously, the dominant grain boundary precipitate changes from the icosahedral phase to the T2 phase below 374F. Three types of strengthening precipitates form in 2090, Al_3Li, Al_2CuLi and Al_2Cu. Because of the low interfacial energy and coherency strain associated with the Al_3Li precipitate, it forms homogeneously at the aging temperatures of this study. As the aging temperature is decreased, the degree of supersaturation and the driving force for nucleation both increase. This results in a decrease in the critical particle radius needed for stable nucleation and an increase in the frequency of nucleation (21). Although the deformation prior to aging does not effect the precipitation of Al_3Li, it has a significant effect on the precipitation of both Al_2CuLi and Al_2Cu, as shown previously.

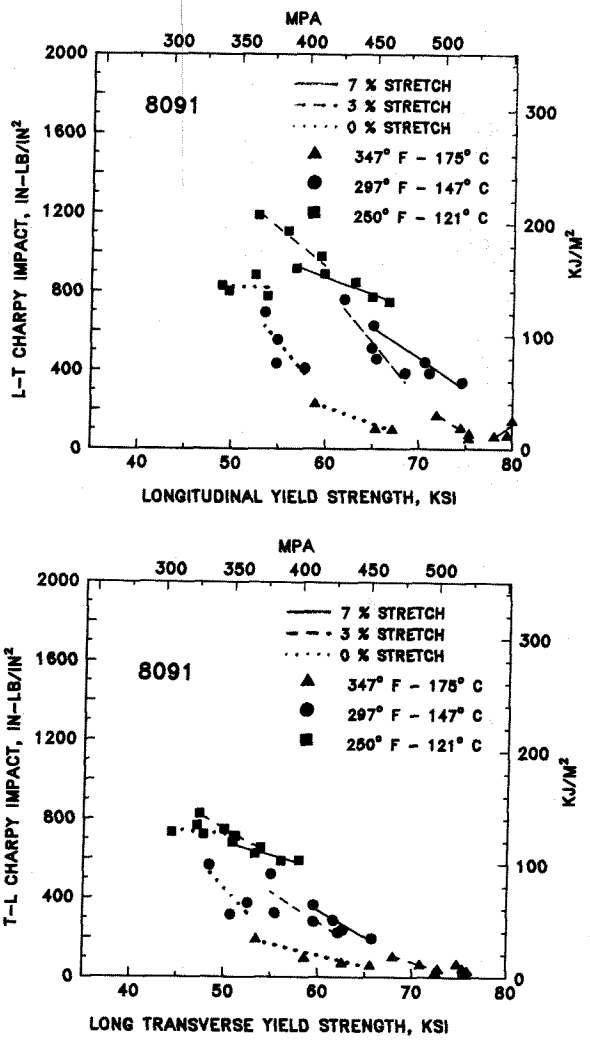

Figure 11. Effect of % stretch and aging practice on the yield strength and Charpy impact energy of 8091 0.50" plate. Plate was solution treated at 1006F. (a) Upper-L, (b) Lower-LT.

Figure 12 shows the effect of both the stretch and aging temperature on the precipitation behavior of alloy 2090. Figure 12a is a bright field TEM showing Al_2CuLi and Al_2Cu precipitates distributed relatively homogeneously throughout the grain in plate that was not stretched prior to aging for 60 hours at 347F. A large precipitate is also observed in the high angle grain boundary. The grain boundary precipitate has denuded the adjacent region of Li resulting in a very

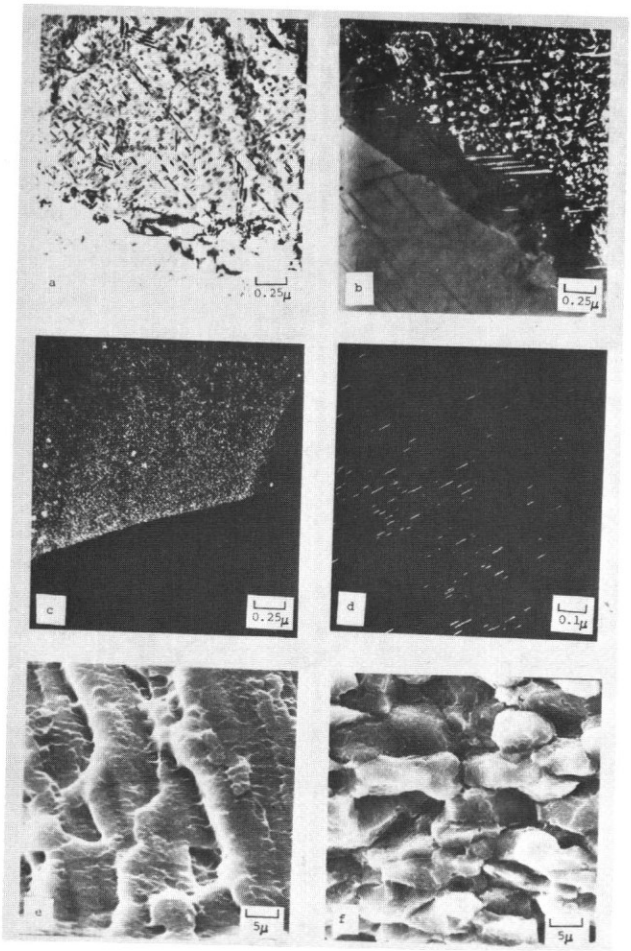

Figure 12. Fine structure and fracture features of 2090 alloy plate. (a) BF-TEM, T1 and Al_2Cu in 0% stretch, 60h at 347F. (b) DF-TEM of (a). (c) and (d) DF-TEM of 7% stretch 60h at 250F showing Al_3Li and T1, respectively. (e) and (f) SEM images of fracture features of 250F and 347F aged plate, respectively.

large Al_3Li PFZ adjacent to the grain boundary, as observed in the dark field TEM of Al_3Li in Figure 12b. Some Al_2CuLi precipitates are also observed in this figure since a Al_2CuLi reflection was near the Al_3Li reflection used to produce the dark field TEM. The precipitate size and distribution were quite different when the alloy was stretched 7% prior to aging and aged for 60 hours at 250F. Figure 12c is a dark field TEM of Al_3Li after this treatment and shows a much finer precipitate and no PFZ adjacent to the high angle grain boundary. The observed difference in the Al_3Li precipitate size and distribution is associated with the lower temperature aging and not the stretch, since dislocations have little or no effect on precipitates that have very low coherency strains and interfacial energies. The Al_3Li precipitation is sufficiently fast and the aging temperature sufficiently low to inhibit nucleation and growth of grain boundary precipitates. The stretch has a significant effect on the size and distribution of the T1 precipitate, as observed in the dark field TEM of Figure 12d of one variant of the T1 phase. The size is very much smaller and the number density very much larger than that observed for the unstretched condition.

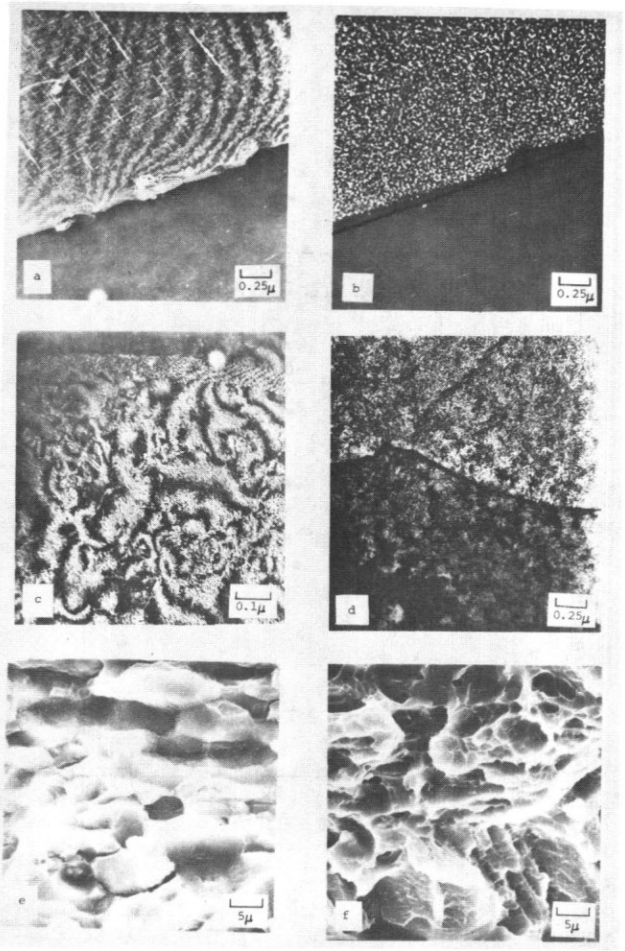

Figure 13. Fine structure and fracture features of 8091 alloy plate. (a) and (b) DF-TEM's of 0% stretch 60h at 347F age, Al_2CuMg and Al_3Li, respectively. (c) and (d) Same as (a) and (b) only 7% stretch and 36h at 250F. (e) and (f) SEM images of fracture features of 347F and 250F aged plate, respectively.

Scanning electron microscopy of the fractured Charpy impact specimens supported the TEM observations. With the 7% stretch, 60 hours at 250F aged plate, the fractures were combinations of flat transgranular shear and intergranular, with the majority of fracture being flat shear, Figure 12e. As the aging temperature was increased, the fractures became largely intergranular, Figure 12f, with dimpling present on the intergranular facets. The dimples are a result of voids nucleating at the grain boundary precipitates and cracks propagating through the PFZ's.

Only two strengthening precipitates were observed in 8091: Al_3Li and Al_2CuMg. The metastable Al_2CuMg has large coherency strains and, as shown previously, it normally nucleates on dislocations similar to the T1 phase. Figure 13a is a dark field TEM showing the Al_2CuMg phase in the 8091 alloy that was not stretched and was aged at the relatively high temperature of 347F. Although the Al_2CuMg precipitates appear to be homogeneously distributed throughout the grains, a large amount of grain boundary precipitate and a very wide PFZ are observed. Figure 13b is a dark field TEM of Al_3Li. A wide Al_3Li PFZ is also observed in this micrograph. In 8091 stretched 3% prior to aging at the intermediate temperature of 297F, some grain boundary precipitation and a narrow PFZ were observed. After this treatment the Al_2CuMg was somewhat finer than observed in Figure 13a. Increasing the stretch to 7% and aging at the same temperature, i.e., 297F, further reduced the amount of grain boundary precipitation and refined both metastable precipitates. As observed for the 2090 alloy, the 7% stretch and 250F age gave the finest precipitate structure and eliminated both grain boundary precipitates and PFZ's, Figures 13c and 13d. All of these samples had been aged to obtain a yield strength of approximately 61 ksi.

The sample that was not stretched and which was aged at the highest temperature had the lowest fracture toughness. During the fracture toughness test, strain was localized in the wide PFZ, voids nucleated at the grain boundary precipitates, and low energy intergranular fracture resulted, Figure 13e. As the stretch prior to aging was increased and the aging temperature decreased, the number and size of grain boundary precipitates were reduced, the PFZ width was reduced, and the matrix precipitate structure was refined. All of these factors aided in homogenizing the deformation, leading to higher energy transgranular fracture, as observed in Figure 13f. This resulted in the observed increase in fracture toughness.

This study clearly shows that the final combination of strength and toughness is very sensitive to the aging temperature, aging time, and degree of stretch prior to aging. Lower aging temperatures yield better combinations of strength and toughness due to the reduction in grain boundary precipitation, and higher stretch levels result in a higher strength for a given toughness due to the refinement of the strengthening precipitate structure.

Acknowledgements

I would like to thank R. F. Ashton of the Reynolds Metals Company and William A. Cassada of the University of Virginia for providing many of the figures used in this manuscript. Support by the U.S. Army Research Office under contract DAAG29-83-K-0038, Dr. Andrew Crowson, Program Director during the preparation of this manuscript is gratefully acknowledged.

References

1. J.S. Ekvall, J.E. Rhodes and G.G. Wald in Design of Fatigue and Fracture Resistant Structures, ASTM STP 761, 1982, p. 328.

2. W.E. Quist, G.H. Harinarayanan and A.L. Wingert in Aluminum-Lithium Alloys II, E.A. Starke, Jr., and T.H. Sanders, Jr., eds., TMS-AIME, Warrendale, PA, 1984, p. 313.

3. E.A. Starke, Jr., T.H. Sanders, Jr., and I.G. Palmer, J. Metals 33 (1981) p. 24.

4. K.K. Sankaran and N.J. Grant, in Aluminum-Lithium Alloys, T.H. Sanders, Jr., and E.A. Starke, Jr., eds., AIME, Warrendale, PA, 1981, p. 205.

5. E.S. Balmuth and R. Schmidt, Aluminum-Lithium Alloys, T.H. Sanders, Jr., and E.A. Starke, Jr., eds., TMS-AIME, Warrendale, PA, 1981, p. 69.

6. G.T. Hahn and A.R. Rosenfield, Metall. Trans. A 6A (1975) p. 653.

7. J.T. Staley, "Properties Related to Fracture Toughness," in ASTM-STP 605, W.R. Warke, V. Weiss and G.T. Hahn, eds., ASTM, 1975, p. 71.

8. Edgar A. Starke, Jr., and Gerd Luetjering in Fatigue and Microstructure, M. Meshii, ed., American Society of Metals, Metals Park, OH, 1979, p. 205.

9. B. Noble and G.E. Thompson, Metal Sci. J. 5 (1971) p. 114.

10. T.H. Sanders, Jr., E.A. Ludwiczak and R.R. Sawtell, Mater. Sci. Engr. 43 (1980) p. 247.

11. E.E. Hornbogen and G. Luetjering in 6th Inter. Conf. on Light Metals, Leoben/Vienna, Austria (1975), Aluminium Verlag, Dusseldorf, 1975, p. 40.

12. I.G. Palmer, R.E. Lewis, D.D. Crooks, E.A. Starke, Jr., and R.E. Crooks in Aluminum-Lithium Alloys II, E.A. Starke, Jr., and T.H. Sanders, Jr., eds., TMS-AIME, Warrendale, PA, 1984, p. 91.

13. Air Force Wright Aeronautical Laboratory Materials Laboratory Contract No. F33615-81-C-5053 with The Boeing Company.

14. P.E. Bretz and R.R. Sawtell in Aluminum-Lithium Alloys III, C. Baker, P.J. Gregson, S.J. Harris and C.J. Peel, eds., The Inst. of Metals, London, 1986, p. 47.

15. M. A. Reynolds, A. Gray, E. Creed, R.M. Jordan and A.P. Titchener in Aluminum-Lithium Alloys III, C. Baker, P.J. Gregson, S.J. Harris and C.J. Peel, eds., The Inst. of Metals, London, 1986, p. 57.

16. R.E. Lewis and E.A. Starke, Jr., in Mechanical Behavior of Rapidly Solidified Materials, Shankar M.L. Sastry and Bruce A. MacDonald, eds., TMS-AIME, Warrendale, PA, 1986, p. 151.

17. I.G. Palmer, R.E. Lewis and D.D. Crooks, in Aluminum-Lithium Alloys, T.H. Sanders, Jr., and E.A. Starke, Jr., eds., TMS-AIME, Warrendale, PA, 1981, p. 241.

18. W.A. Cassada, G.J. Shiflet, and E.A. Starke, Jr., Scripta Met. 20, 1986, p. 751.

19. W.A. Cassada, G.J. Shiflet, and E.A. Starke, Jr., "Characterization of Two Grain Boundary Precipitates in Al-Li-Cu Alloys with Electron Micro-Diffraction," Proceedings of the International Conference on Aluminum Alloys, Their Physical and Mechanical Properties, E.A. Starke, Jr., and T.H. Sanders, Jr., eds., Engineering Materials Advisory Services, Ltd., Warley, United Kingdom (in press).

20. J.C. Williams and E.A. Starke, Jr., in Deformation, Processing and Structure, George Krauss, ed., ASM, Metals Park, OH, 1984, p. 279.

21. R.F. Ashton, D.S. Thompson, E.A. Starke, Jr., and F.S. Lin in Aluminum-Lithium Alloys III, C. Baker, P.J. Gregson, S.J. Harris, and C.J. Peel, eds., The Inst. of Metals, London, 1986, p. 66.